Exactly Solving the Weighted Time/Fuel Optimal Control of an Undamped Harmonic Oscillator

Marcelo Lopes de Oliveira e Souza*
Instituto de Pesquisas Espaciais, São Josē dos campos, Brazil

The exact solution to the problem of the weighted time/fuel optimal control of an undamped harmonic oscillator with one bounded control and any initial state is summarized. The motivation is the possibility of improvements in the final behavior of trajectories produced by Vander Velde's designs for on/off controls of large space structures, by replacing his approximate solution with the exact one. This includes: 1) the development and extensive study of the first-order necessary conditions; 2) investigations of the existence, normality, uniqueness, and determination of the extremals and the optimal solution; and 3) numerical comparisons between the approximate and exact solutions according to three criteria, including those improvements. It is found that the extremals (solution) exist(s), are (is) normal, can be nonunique but in a finite number (is unique), can be determined by an algorithm based on items 1 and 2, and seems to improve the final behavior of the controller.

Nomenclature

$a(.)$ = backward phase angle of $\boldsymbol{p}_{F1}(.)$
a_j = $a(\tau_j)$ = jth backward switching angle of $u(.)$
b_{F1},b = fuel weight for $u(.)$ in $J_{F1}[\boldsymbol{y}_{F1_0},u(.)]$
b_j = fuel weight for the jth component of $\boldsymbol{u}(.)$ in $J[\boldsymbol{y}_0,\boldsymbol{u}(.)]$
c_{F1},c = second row of $u(.)$ matrix coefficient
$\boldsymbol{c}_j^T$ = jth row of $\boldsymbol{u}(.)$ matrix coefficient
$d_{F1}(.)$ = scalar input to the $u(.)$ relay in problem 2
$d_R(.)$ = scalar input to the $u(.)$ relay in the rigid subproblem
$\boldsymbol{d}(.)$ = vector input to the $\boldsymbol{u}(.)$ relays in problem 1
D_u = $\{t_1, \ldots, t_j, \ldots, t_s\}$
$H_{F1}(.,.,.)$ = Hamiltonian in problem 2
$J_{F1}(.,.)$ = cost in problem 2
$J(.,.)$ = cost in problem 1
k = (even) number of components of $\boldsymbol{y}(.)$
l = number of components of $\boldsymbol{u}(.)$
m = number of on arcs between the (m,n) arc and the origin in problem 2
n = number of off arcs between the (m,n) arc and the origin in problem 2
$n_{\max}$ = maximum number of extremal switching lines to be tested for intersection in the algorithm solving problem 2
o = y_3 coordinate of the (m,n) arc center in the $\boldsymbol{y}_{F1}$ phase plane
P = period of $\boldsymbol{p}_{F1}(.)$
$\boldsymbol{p}_{F1(.)}$ = costate trajectory in problem 2, with coordinates p_3 and p_4
r = radius of $\boldsymbol{p}_{F1}(.)$
r_f = relative error in t_f^a with respect to t_f^o
r_n = relative error in t_{on}^a with respect to t_{on}^o
r_J = relative error in J_{F1}^a with respect to J_{F1}^o
S^2 = set of all piecewise smooth vector functions $\boldsymbol{s}$: $[0,t_f] \to R^2$
s = number of switching instants of $u(.)$
$\boldsymbol{s}(.)$ = an element of S^2
t = forward time
t_j = jth forward switching instant of $u(.)$
t_{on} = total amount of time during which $u(.)$ is on
U = set of all piecewise continuous scalar functions u: $[0,t_f] \to U$
U = $\{-um,0,um\}$
$u(.)$ = scalar control function in problem 2
$\boldsymbol{u}(.)$ = vector control function in problem 1, with coordinates $u_1, \ldots, u_l$
um = maximum value for $u(.)$
um_j = maximum value for $u_j(.)$
$\boldsymbol{y}_{F1}(.)$ = state trajectory in problem 2, with coordinates y_3 and y_4
$\boldsymbol{y}(.)$ = state trajectory in problem 1, with coordinates $y_1, \ldots, y_k$
z = (m,n) arc radius squared $[h_{m+n}(q)]$ minus threshold $(m+n-1)^2$
μ = control magnitude when the minimum principle of Pontryagin can be satisfied by more than one control value
θ = half the angle during which the problem 2 control is on in each half-cycle of the oscillation
τ = backward time as defined in convention 2
τ_j = jth backward switching instant of $u(.)$
ω_1,ω = angular frequency in problem 2
σ_j = attenuation in the jth flexible subproblem

Superscripts

a = approximate value
e = extremal value
o = optimal value

Subscripts

f = final mode
$F1$ = first flexible mode
j = switching mode
R = rigid mode
0 = initial mode

Introduction

RECENTLY, Vander Velde and He[1] proposed a new design method for large space structure (LSS) control systems using on/off thrusters based on their approximate solution to the problem of the weighted time/fuel optimal control of the linear dynamic model of a flexible spacecraft with many bounded controls and any initial state (problem 1). Despite its practical advantages,[1] one of its disadvantages resided in its final behavior: a final cycle with non-negligible dimensions.

Received Jan. 7, 1987; revision received Sept. 14, 1987.

*Assistant Researcher, Department of Control and Guidance. Member AIAA.

This called for studies aiming at its reduction/suppression. One possibility considered by the author consists of: 1) exactly solving the problem of the weighted time/fuel optimal control of an undamped harmonic oscillator with one bounded control and any initial state (problem 2), and 2) substituting it for the approximate solution used in Ref. 1. The results of this conjecture were obtained by Souza[2] and are summarized in this work.

Weighted time/fuel optimal control problems have been studied for a long time, but to a lesser extent than their time, fuel, or energy counterparts.[3,4] Particularly, problem 2 (with restricted initial state) was stated (but not solved) by Athans and Falb (Ref. 3, p. 749, exercise 8-50). An approximate solution to it (valid for any initial state) was presented by Vander Velde and He[1] as part of their design method.

In this work, the exact solution to problem 2 is summarized. The motivation is the possibility of improvements in the final behavior of trajectories produced by Vander Velde's designs for on/off controls of large space structures by replacing his approximate solution with the exact one. This includes: 1) the development and extensive study of the first-order necessary conditions; 2) investigations on the existence, normality, uniqueness, and determination of the extremals and the optimal solution; and 3) numerical comparisons between the approximate and exact solutions according to three criteria, including those improvements. It is found that the extremals (solution) exist(s), are (is) normal, can be nonunique but in a finite number (is unique), can be determined by an algorithm based on items 1 and 2 (and seems to improve the final behavior of the controller).

Statement of the Problem

Let us state the control problem (problem 2) as follows:

Globally minimize

$$J_{F1}[\boldsymbol{y}_{F1_0},u(.)] = \int_0^{t_f} (1 + b_{F1} \cdot |u(t)|\,|u(t)|) \cdot \mathrm{d}t$$

with respect to $u(.) \in \mathcal{U}$ where $\mathcal{U}$ is the set of all piecewise continuous scalar functions u: $[0,t_f] \to U$ in which $U = \{-um, 0, um\}$ [that is, $u(.)$ may have a finite number of points of discontinuity of the first kind $t_j \in (0,t_f)$, which means that $\exists \lim u(t) \in R$ when $t \to t_j^-$ and $\exists \lim u(t) \in R$ when $t \to t_j^+$. The set of all t_j can be called D_u]; $u(.)$ is continuous from below at any t_j, continuous at 0 and at t_f, as assumed by Pontryagin et al. (Ref. 5, pp. 10–11), and subject to $\boldsymbol{y}_{F1}(.) \in \mathcal{S}^2$, where $\boldsymbol{y}_{F1}(.) = [y_3(.), y_4(.)]^T$ and $\mathcal{S}^2$ is the set of all piecewise smooth vector functions $\boldsymbol{s}$: $[0,t_f] \to R^2$, such that

$$\forall t \in [0,t_f] - D_u$$

$$\begin{bmatrix} \dot{y}_3(t) \\ \dot{y}_4(t) \end{bmatrix} = \begin{bmatrix} 0 & \omega_1 \\ -\omega_1 & 0 \end{bmatrix} \begin{bmatrix} y_3(t) \\ y_4(t) \end{bmatrix} + \begin{bmatrix} 0 \\ c_{F1} \end{bmatrix} \cdot u(t)$$

$$\boldsymbol{y}_{F1}(0) = \boldsymbol{y}_{F1_0}, \quad \boldsymbol{y}_{F1}(t_f) = \boldsymbol{0} \tag{1}$$

where $\boldsymbol{y}_{F1_0} = (y_{3_0}, y_{4_0})^T$, given

$$\boldsymbol{y}_{F1_0} \in R^2 - \{\boldsymbol{0}\}, \quad b_{F1} \in (0,\infty), \quad c_{F1} \in R^+$$

$$um \in R^+, \quad \omega_1 \in R^+ \tag{2}$$

First-Order Necessary Conditions

The Hamiltonian for problem 2 is the function

$$H_{F1}\colon R^2 \times R^2 \times U \to R\colon \forall (\boldsymbol{p}_{F1}, \boldsymbol{y}_{F1}, u) \in R^2 \times R^2 \times U$$

$$H_{F1}(\boldsymbol{p}_{F1}, \boldsymbol{y}_{F1}, u) = 1 + \omega_1 \cdot (p_3 \cdot y_4 - p_4 \cdot y_3) + b_{F1} \cdot |u| + c_{F1} \cdot p_4 \cdot u \tag{3}$$

where $\boldsymbol{p}_{F1} = (p_3, p_4)^T$ and $\boldsymbol{y}_{F1} = (y_3, y_4)^T$.

The first-order necessary conditions for problem 2, as prescribed by the minimum principle of Pontryagin (see Ref. 5, theorem 1, p. 19) are as follows.

If an optimal control $u^o(.)$ [and the correspondent $t_f^o, \boldsymbol{y}_{F1}^o(.)$] exists, then it belongs to the set of all extremal controls $u^e(.)$ [and the correspondent $t_f^e, \boldsymbol{y}_{F1}^e(.)$] defined by

1) $$\boldsymbol{p}_{F1}^e(.) \in \mathcal{S}^2\colon \boldsymbol{p}_{F1}^e(.) \neq \boldsymbol{0} \tag{4}$$

where $\boldsymbol{p}_{F1}^e(.) = [p_3^e(.), p_4^e(.)]^T$ and $\mathcal{S}^2$ is defined as before.

2) $$\forall t \in [0,t_f^e] - D_u$$

$$\begin{bmatrix} \dot{p}_3^e(t) \\ \dot{p}_4^e(t) \end{bmatrix} = \begin{bmatrix} 0 & \omega_1 \\ -\omega_1 & 0 \end{bmatrix} \begin{bmatrix} p_3^e(t) \\ p_4^e(t) \end{bmatrix} \tag{5}$$

where $\boldsymbol{p}_{F1}^e(0)$ and $\boldsymbol{p}_{F1}^e(t_f^e)$ are not known for a given $\boldsymbol{y}_{F1_0}$.

3) $$\forall t \in [0,t_f^e],\ d_{F1}^e(t) = c_{F1} \cdot p_4^e(t) \tag{6}$$

Also:

If $0 \leqq |d_{F1}^e(t)| < b_{F1}$, then $u^e(t) = 0$.
If $|d_{F1}^e(t)| = b_{F1}$, then $u^e(t) = -\mu \cdot \text{sign}\,[d_{F1}^e(t)]$, $\mu \in \{0, um\}$.
If $b_{F1} < |d_{F1}^e(t)| < \infty$, then $u^e(t) = -um \cdot \text{sign}[d_{F1}^e(t)]$.

4) $$\forall t \in [0,t_f^e]$$

$$1 + \omega_1 \cdot [p_3^e(t) \cdot y_4^e(t) - p_4^e(t) \cdot y_3^e(t)] + b_{F1} \cdot |u^e(t)| + d_{F1}^e(t) \cdot u(t) = 0 \tag{7}$$

To study these conditions extensively, let us adopt the following conventions:

1) Simplification of notation: $b = b_{F1}$, $c = c_{F1}$, $\omega = \omega_1$, and all superscripts e are deleted.

2) Change of independent variable: $t\colon [\tau_0,\tau_f] \to [0,t_f]$: $\forall \tau \in [\tau_0,\tau_f]$, $t = t_f - \tau$, where $\tau_0 = 0$ and $\tau_f = t_f$. The notations for the functions of time will be preserved, but their arguments will be shortened from $t = (t_f - \tau)$, $t_f = (t_f - \tau_0)$, $0 = (t_f - \tau_f)$ to τ, τ_0, τ_f, respectively, τ will be called backward time.

By integrating the costate $\boldsymbol{p}_{F1}(.)$ and state $\boldsymbol{y}_{F1}(.)$ differential equations (5) and (1) in backward time τ, we get the trajectories shown in Figs. 1 and 2, respectively. There (and from now on), $u(\tau_0) = um$ because the other possibility $[u(\tau_0) = -um]$ admitted by Eq. (7) produces symmetrical results. They illustrate that:

1) For a given $\boldsymbol{y}_{F1_0} \in R^2 - \{\boldsymbol{0}\}$, it is sufficient to find the candidates (=extremals) $u(\tau_0) \in \{-um, um\}$, $p_3(\tau_0) \in R$, and $\tau_f \in R^+$ to determine the corresponding candidates $\boldsymbol{p}_{F1}(.)$, $u(.)$, $\boldsymbol{y}_{F1}(.)$, and $J_{F1}[\boldsymbol{y}_{F1_0}, u(.)]$ and then to select the minimum cost $u(.)$. This is done by an algorithm[2] based on this work.

2) $d_{F1}(.)$ cannot stay constant, particularly at b. This leads to:

Conclusion 1. If an extremal control exists, then it is normal, i.e., nonsingular.

3) τ_f and the $d_{F1}(.)$ period are finite, thus producing a finite number s of backward switching instants τ_j and angles a_j, $j \in \{1, \ldots, s\}$ (the $j = s + 1$ values are virtual). This leads to:

Conclusion 2. If $\tau_1, \ldots, \tau_s$ exist, then on $[\tau_0,\tau_1], \ldots, [\tau_s,\tau_{s+1}]$, $u(\tau)$ cyclically is equal to $um, 0, -um, 0$. These on or off time intervals, respectively, satisfy

$$0 < (\tau_1 - \tau_0) < (\tau_3 - \tau_2) = (\tau_5 - \tau_4) = \cdots = \frac{2 \cdot \theta}{\omega} < \frac{P}{2}$$

or

$$0 < (\tau_2 - \tau_1) = (\tau_4 - \tau_3) = \ldots = \frac{P}{2} - \frac{2 \cdot \theta}{\omega}$$

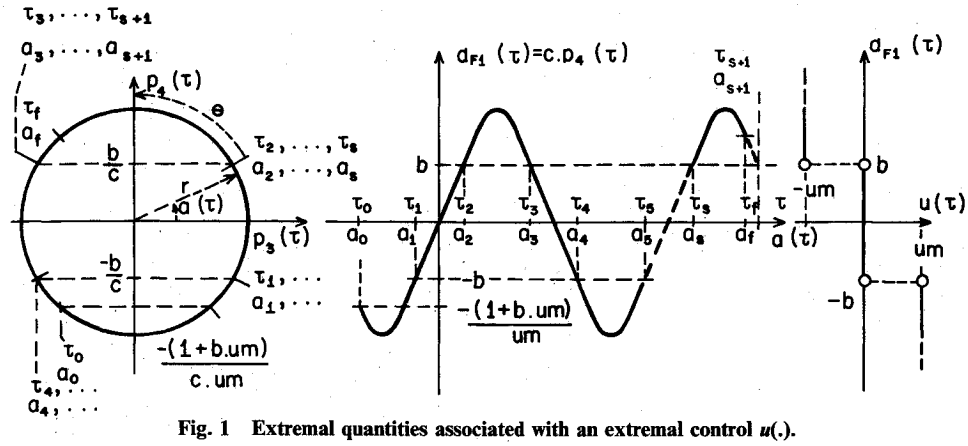

Fig. 1 Extremal quantities associated with an extremal control $u(.)$.

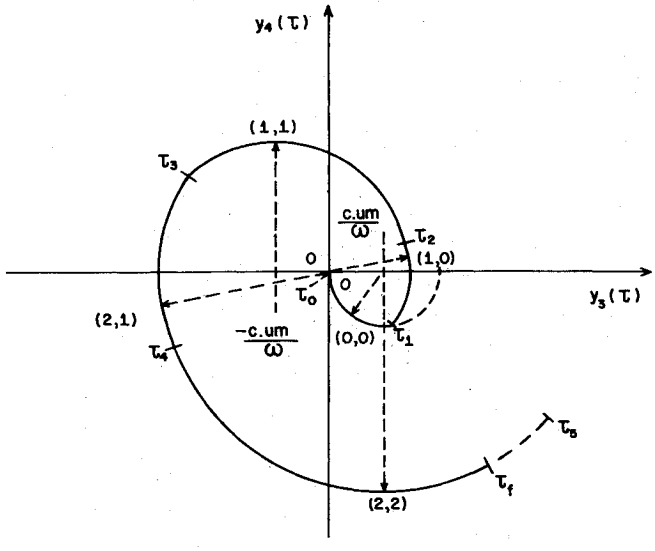

Fig. 2 First five arcs of an extremal state trajectory $y_{F1}(.)$

Also, $[\tau_s,\tau_f] \subset [\tau_s,\tau_{s+1}]$ and $[\tau_s,\tau_f]$ is on or off, respectively, satisfying

$$0 < (\tau_f - \tau_s) \leqq (2 \cdot \theta)/\omega$$

or

$$0 < (\tau_f - \tau_s) \leqq (P/2) - (2 \cdot \theta)/\omega$$

If $\tau_1, \ldots, \tau_s$ do not exist, then on $[\tau_0,\tau_f]$, $u(\tau) = um$, and $0 < (\tau_f - \tau_0) < 2 \cdot \theta/\omega$.

By repeating that integration for the same b, c, um, and ω, $u(\tau_0) = um$ (the $-um$ results are symmetric), many $p_3(\tau_0) \in R$, and a given $\tau_f \in R^+$, we can draw the correspondent extremal switching lines in the y_{F1} phase plane by plotting $y_{F1}(\tau)$ whenever $|d_{F1}(\tau)| = b$. Then, for increasing b, we get a sequence of sets of switching lines in the phase plane showing the influence of weighting on the control in the cost function. Figures 5.7 a, c, e, and h of Brown[6] were obtained this way using $b = 0, 0.1, 1.0, 10$, respectively, and $c = 1$, $um = 1$, $\omega = 1$ rad/s. They illustrate that:

1) If $b = 0$, then problem 2 reduces to its time-optimal counterpart, first solved by Bushaw.[7] From any initial state $y_{F1_0} \in R^2 - \{0\}$—e.g., $y_{F1_0} = P(3.3; -3.3)$ in Fig. 3—there is one and only one (normal) extremal state trajectory $y_{F1}(.)$ and the correspondent control $u(.)$. Thus, these are also optimal.

2) If $b > 0$, then each extremal switching line of item 1 splits in two [to admit $u(\tau) = 0$ arcs] and evolves to a semicrescent with concavity and vertices directed toward the origin, partially involving the previous one. Then, for large $b \cdot um$ or large $\|y_{F1_0}\|$—e.g., $b \cdot um = 10$ and $y_{F1_0} = P(1; 1.2)$ in Fig. 4—there are many (normal) extremal state trajectories $y_{F1}(.)$ and the correspondent controls $u(.)$. So, to find the optimal ones, we must find all of them, compute their costs, and select the minimum cost (cheapest) ones. This has been done[2] according to the following steps:

1) Extensively study those first-order necessary conditions, particularly:

a) Express $y_{F1}(\tau_f)$, given $u(\tau_0)$, $p_3(\tau_0)$, and τ_f. Use m and n, which are and the number of on and off arcs between the (m,n) arc and the origin in problem 2. See Fig. 2.

b) From step 1a express $\cos(\omega \cdot \tau_f)$ and $\sin(\omega \cdot \tau_f)$, given $y_{F1}(\tau_f)$, $u(\tau_0)$, and $p_3(\tau_0)$.

c) From step 1b, obtain, solve, and discuss the equation for $p_3(\tau_0)$, given $y_{F1}(\tau_f)$ and $u(\tau_0)$.

d) With the solution of step 1c, express all other quantities (specially τ_f, τ_{on} and J_{F1}), given $u(\tau_0)$, $p_3(\tau_0)$, and τ_f.

e) From step 1a, obtain and study all properties of the parametric equations of the extremal switching lines $y_{F1}(\tau_j)$, given $u(\tau_0)$ and j, the parameter being $p_3(\tau_0)$.

2) Investigate the questions of existence, normality, uniqueness, and determination of the extremal and optimal $u(.)$ and $y_{F1}(.)$.

3) From steps 1 and 2, construct an algorithm (presented in Appendix A of Ref. 2) to determine the extremal and the optimal $u(.)$ and $y_{F1}(.)$ by comparing y_{F1_0} with those extremal switching lines, finding all of those extremals, computing their costs, and selecting the minimum cost (cheapest) ones. For example, for the data and point in Fig. 4, it produces the output in Table 1.

Existence, Normality, Uniqueness, and Determination of Its Extremals and Its Solution

The main conclusions about these questions are drawn from Ref. 2. In addition to those summarized in the previous section, they are:

Conclusion 3. The problem 2 extremal controls exist, are normal, can be nonunique (but in a finite number), and can be determined by that algorithm.

Conclusion 4. The problem 2 optimal control exists, is normal, is unique, and can also be determined by that algorithm

Conclusion 5. Such algorithm can synthesize $u^o(t)$ as a function of $y^o(t)$ only, because y_{F1_0} is arbitrary and problem 2 is time invariant. Thus, it can be used to produce closed-loop control. It is a numerical solution in that closed-form expressions defining all extremals originating at a given point are evaluated and the lowest cost extremal is selected as the optimal solution. In this sense, it is the exact solution to problem 2. It is numerically compared with the Vander Velde solution to problem 2 in the following sections.

Comparisons with the Vander Velde Solution to Problem 2

The Vander Velde solution to problem 2 is obtained by particularizing his solution to the first constrained flexible sub-

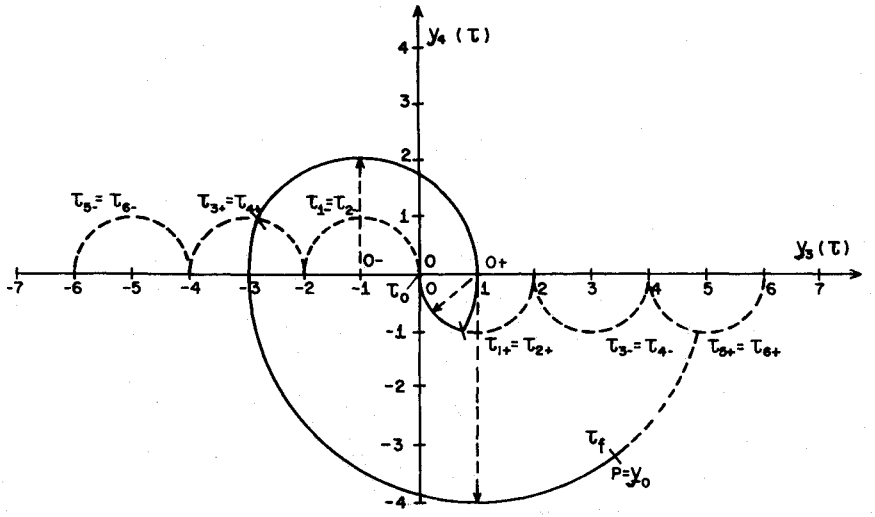

Fig. 3 Unique extremal trajectory $y_{F1}(.)$ associated with an initial state $y_{F1_0} = P$, for $b = 0$.

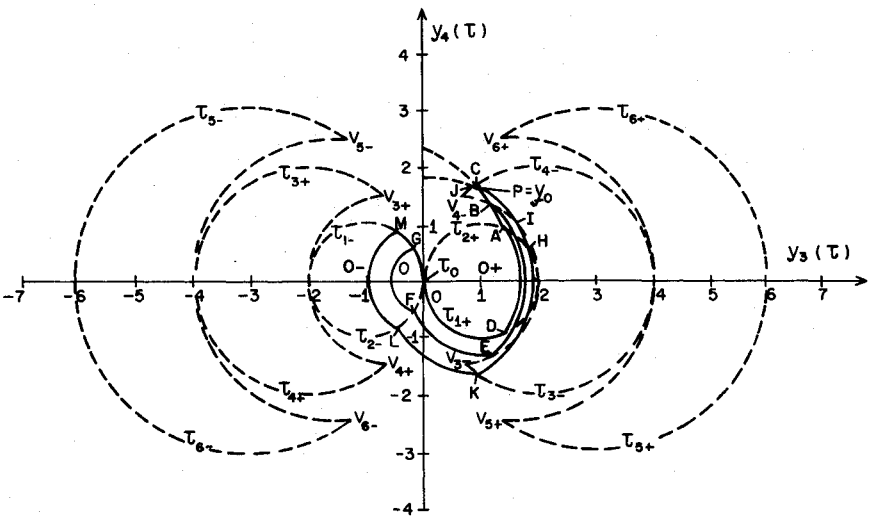

Fig. 4 Three extremal trajectories $y_{F1}(.)$ associated with an initial state $y_{F1_0} = P$, for $b > 0$.

problem[2] to the undamped ($\sigma_1 = 0$) case and by transforming it from (Y_3, Y_4) to (y_3, y_4) coordinates [to obtain 0 in place of r_{F1}, the $u(t)$ coefficient in $\dot{Y}_3(t)$].

In his solution to problem 1, he approximates the problem 2 constate vector by the gradient of a cost function $J^a_{F1}(.)$ deduced through energy considerations. This produces the following expressions for the approximate t_f, t_{on}, and J_{F1}:

$$t^a_f(y_{F1}) = \frac{\pi/2}{c \cdot um \cdot \sin\theta^a} \cdot \sqrt{y_3^2 + y_4^2}$$

$$t^a_{on}(y_{F1}) = \frac{\theta^a}{c \cdot um \cdot \sin\theta^a} \cdot \sqrt{y_3^2 + y_4^2}$$

$$J^a_{F1}(y_{F1}) = t^a_f(y_{F1}) + b \cdot um \cdot t^a_{on}(y_{F1})$$

$$= \frac{(\pi/2 + b \cdot um \cdot \theta^a)}{c \cdot um \cdot \sin\theta^a} \cdot \sqrt{y_3^2 + y_4^2}$$

$$= \frac{b}{c \cdot \cos\theta^a} \cdot \sqrt{y_3^2 + y_4^2} \quad \text{if } b > 0$$

where θ^a represents one-half of the angle during which the control is on in each half-cycle of the oscillation. It is given by the unique solution to the equation (used to arrive at the last of the previous expressions),

$$b \cdot um - \left(\frac{\pi}{2} + b \cdot um \cdot \theta^a\right) \cdot \text{ctg}\theta^a = 0, \theta^a \in \left(0, \frac{\pi}{2}\right)$$

which shows that θ^a is a monotonically decreasing function of $b \cdot um$. These expressions can also be deduced through other considerations, as shown in Appendix B of Ref. 2.

The comparison of this approximate solution with the previously obtained exact solution shows that: its main advantage resides in its algebraic and simple form, which is extremely convenient for algebraic or numerical work; its main disadvantage consists of its inverse-with-radius errors, which prevent any state trajectory $y_{F1}(.)$ from reaching the origin **0** optimally. These differences and their effects on problems 1 and 2 state trajectories are further clarified in the remainder of this section are in the following one.

A first criterion for comparing the two solutions is the evaluation of the relative errors in t^a_f, t^a_{on}, and J^a_{F1}, with respect to t^o_f, t^o_{on}, and J^o_{F1}, respectively, at many points y_{F1}. They are defined by

$$r_f(y_{F1}) = \frac{t^a_f(y_{F1})}{t^o_f(y_{F1})} - 1$$

$$r_n(y_{F1}) = \frac{t^a_{on}(y_{F1})}{t^o_{on}(y_{F1})} - 1$$

$$r_J(y_{F1}) = \frac{J^a_{F1}(y_{F1})}{J^o_{F1}(y_{F1})} - 1$$

respectively. This provides a local idea of the differences between those solutions.

Table 2 presents the auxiliary quantities and relative errors for the point and set of parameters listed in Table 1. The

Table 1 Extremal and optimal quantities associated with $y_{F1_0} = P$ in Fig. 4[a]

m	n	z	$u(t_f)$	$p_3(t_f)$	$p_4(t_f)$	θ, rad	t_f, s	t_{on}, s	J
1[b]	1	4.440000	−1	−10.77067	−11.00000	0.8637910	3.197433	1.783422	21.03165
2	2	−3.560000	−1	−8.873020	11.00000	0.7847235	4.914271	1.769980	22.61407
2	1	−1.560000	0	2.222229	11.00000	0.4710571	5.844863	1.612509	21.96996

[a]$b = 10$, $c = 1$, $um = 1$, $\omega = 1$ rad/s, $y_3(t_0) = 1.000000$, $y_4(t_0) = 1.200000$, $n_{max} = 5$, $\theta^a = 0.7200152515$ rad. [b]Optimal.

Table 2 Auxiliary quantities and relative errors in t_f^a, t_{on}^a, J_{F1}^a for the data in Table 1

t_f, s	t_{on}, s	J
3.721075[a]	1.705651	20.77759
3.197433[b]	1.783422	21.03165
16.37694[c]	−4.360766	−1.208007

[a]Approximate. [b]Optimal. [c]Relative error, %.

magnitude of r_f is much greater than that of r_n. However, their signs are different and, since t_f and t_{on} have weights 1 and 10 in the expression of J_{F1}, the relative error in the cost is much smaller. Appendix C of Ref. 2 contains a much more extensive table of similar quantities and errors for many regularly spaced points around the origin and three sets of parameters. Its analysis suggests the following.

Conclusion 6. r_f, r_n, and r_J vary inversely with $b \cdot um$ and $\sqrt{y_3^2 + y_4^2}$, reflecting the dependence of the approximate solution on the number of $y_{F1}(.)$ turns around the origin. That is, the solution is good (bad) for large (small) $b \cdot um$ and (or) points far from (close to) the origin. For large (small) $b \cdot um$, r_f has magnitude larger (smaller) than r_n and an opposite sign in such a way as to produce a much smaller magnitude for r_J. This reflects the minimization of J_{F1}^a (and not of t_f^a or t_{on}^a separately) with respect to the θ^a included in that solution.

A second criterion for comparing the two solutions is the simultaneous plot of the respective problem 2 state trajectories, $y_{F1}^a(.)$ and $y_{F1}^o(.)$ for some initial states y_{F1_0} and sets of parameters. Each $y_{F1}(.)$ is obtained by numerically integrating Eq. (1) using the correspondent synthesized control $u(.) = f[y_{F1}(.)]$, with the same initial state y_{F1_0}, from $t_0 = 0$ until the optimal final time t_f^o associated with y_{F1_0}. This provides a global idea of the differences between those solutions. This also provides a decisive check on the exact solution, namely, the agreement of the numerically integrated $y_{F1}^o(.)$ with the algorithm predictions of it.

Figure 5 contains the $y_{F1}^a(.)$ and $y_{F1}^o(.)$, respectively denoted by AP and EX, correspondent to the data and predictions of Table 3. In Fig. 5, $y_{F1}(t_0) = y_{F1_0}$ was chosen with $m = 8$, $n = 7$, $\tau_f = t_f = 23.6$ s, $p_3(\tau_0) = p_3(t_f) = 0$, $p_4(\tau_0) = p_4(t_f) = (1 + b \cdot um)/c \cdot um$; i.e., $u(\tau_0) = u(t_f) = -um$. The appearance of this candidate among those in Table 3 provides an additional check on the algorithm. However, this does not mean that such a candidate is unique or optimal. Besides this, Fig. 5 shows that $y_{F1}^a(.)$ and $y_{F1}^o(.)$ remain coincident while they are far from the origin. However, as they approach it, these trajectories separate and diverge: the second one goes to **0**, but the first one does not, moving instead in an erratic way close to it. In particular, Fig. 5 clearly shows the perfect agreement of the integrated $y_{F1}^o(.)$ with the predictions of Table 3 with regard to the number and sequence of arcs, initial and final control and state values, etc. This and additional simulations presented in Ref. 2 suggest the following:

Conclusion 7. The global effects of the differences between the approximate and the exact solutions to problem 2 on its state trajectory are quantitatively negligible (qualitatively important) for large (small) $b \cdot um$ and (or) regions far from (close to) the origin. The exact trajectory agrees with the algorithm predictions, particularly going to **0** at t_f^o. The approximate one does not, remaining close to **0** instead. So, in applications where each control value $u(t)$ must be efficiently computed (e.g., in real time with high ω), a suboptimal but

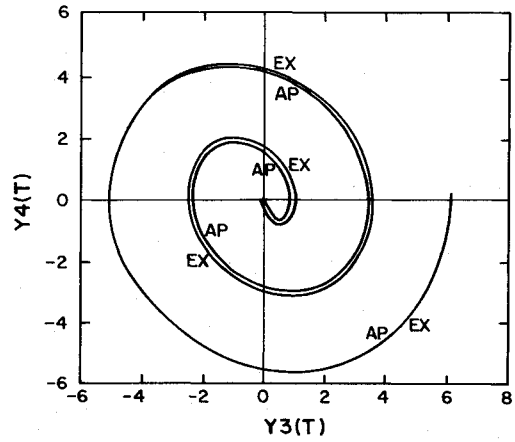

Fig. 5 Approximate (AP) and exact (EX) problem 2 state trajectories $y_{F1}^a(.)$ and $y_{F1}^o(.)$ for the data in Table 3.

practical scheme is to use the approximate solution while the state is far from the origin, and to switch to the exact one when the state becomes close to **0**.†

On the other hand, in the undamped version of problem 1, if the control $u(.)$ had the same number of components l as the number of modes $k/2$ and if each of these were driven by one and only one of the controls through its second coordinate, then the exact solutions to problem 2 and to its rigid counterpart would allow for driving y to **0** exactly. However, this is neither a general nor a practical situation, because $l = k/2$ and k (then l) can be very large in practical applications, greatly increasing the weight, unreliability, cost, etc., of the correspondent implementation; and the $u(.)$ matrix coefficient C has a very special form that requires sophisticated actuators in critical locations, resulting in similar penalties.

Improvements in the Vander Velde Solution to Problem 1

The basic motivation for obtaining the exact solution to problem 2 is the hope for improvements in the Vander Velde solution to problem 1 by replacing his approximate solution to problem 2 with the exact one. Such improvements would then enhance the importance of the exact solution. This suggests the conditions described in this section.

A third criterion for comparing the two solutions is the simultaneous plot of the respective problem 1 state trajectories $y^a(.)$ and $y^{ex}(.)$ for some initial states y_0 and sets of parameters. Each $y(.)$ is obtained by numerically integrating its differential equation as driven by the Vander Velde control logic (including the approximate or the exact solution to problem 2), with the same initial state y_0, from $t_0 = 0$ until both trajectories cease approaching the origin. This provides a combined idea of the differences between those solutions.

Figure 6 contains the $y^a(.)$ and $y^{ex}(.)$, respectively denoted by AP and EX, correspondent to the data in Table 4. These belong to the simplest nontrivial system, namely, that with one rigid mode and one undamped flexible mode driven by one scalar

†Theoretically, $y_{F1}^a(\cdot)$ ends sliding along one of the (straight) switching lines of the Vander Velde solution to problem 2 and then converging asymptotically toward the origin according to an exponential law. However, numerically, this does not happen due to the nonzero integration step and to the errors of the integration algorithm.

Table 3 Extremal and optimal quantities associated with $y_{F1_0} = P$ in Fig. 5[a]

m	n	z	$u(t_f)$	$p_3(t_f)$	$p_4(t_f)$	θ, rad	t_f, s	t_{on}, s	J
4	3	3.057846	0	11.93699	11.00000	0.9070771	11.85517	7.17566	83.61282
5[b]	4	−24.94215	0	−6.841495	−11.00000	0.6888736	14.72943	6.756269	82.29213
5	4	−24.94215	0	11.33717	−11.00000	0.8853108	13.37031	7.167305	85.04337
6	5	−60.94215	0	4.360622	11.00000	0.5640275	17.69321	6.581720	83.51041
6	5	−60.94215	0	−62.62824	11.00000	0.6599561	16.79733	6.741941	84.21675
7	6	−104.9422	0	−2.522186	−11.00000	0.4819419	20.68343	6.490638	85.58981
7	6	−104.9422	0	3.633164	−11.00000	0.5291731	20.13867	6.560243	85.74110
8	7	−156.9422	0	0.000000	11.00000	0.4296996	23.60000	6.445494	88.05494
8	7	−156.9422	0	−0.7450564	11.00000	0.4346614	23.53234	6.452291	88.05526

[a] $b = 10$, $c = 1$, $um = 1$, $\omega = 1$ rad/s, $y_3(t_0) = 6.247901$, $y_4(t_0) = 0.1469043$, $n_{max} = 8$, $\theta^a = 0.7200152515$ rad. [b] Optimal.

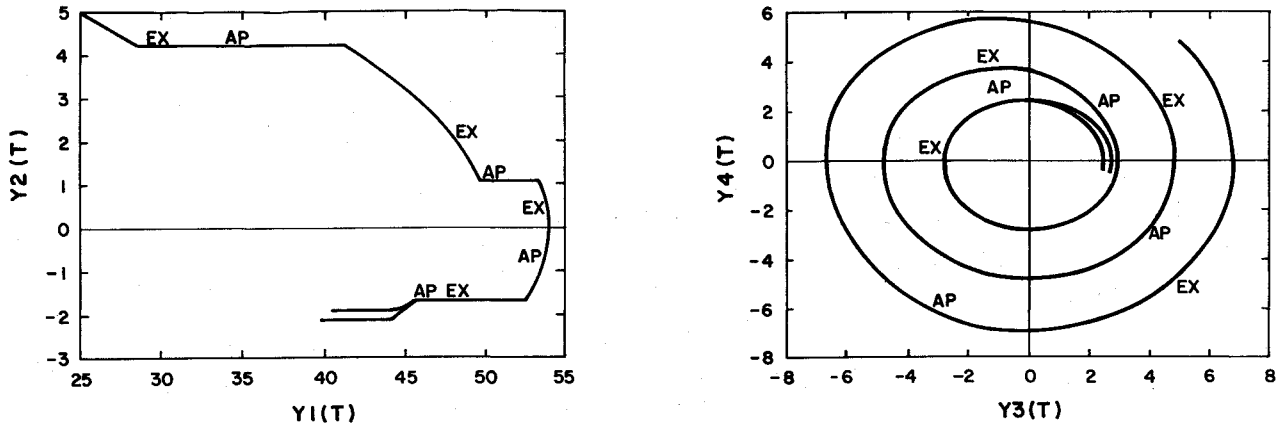

a) $t \in [0.00, 20.00]$ s

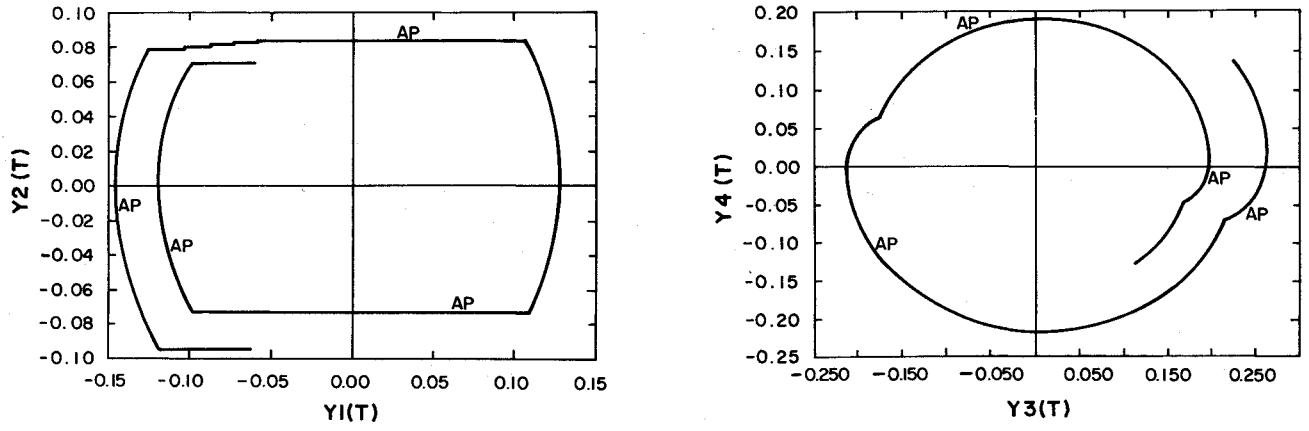

b) $t \in [79.97, 90.00]$ s

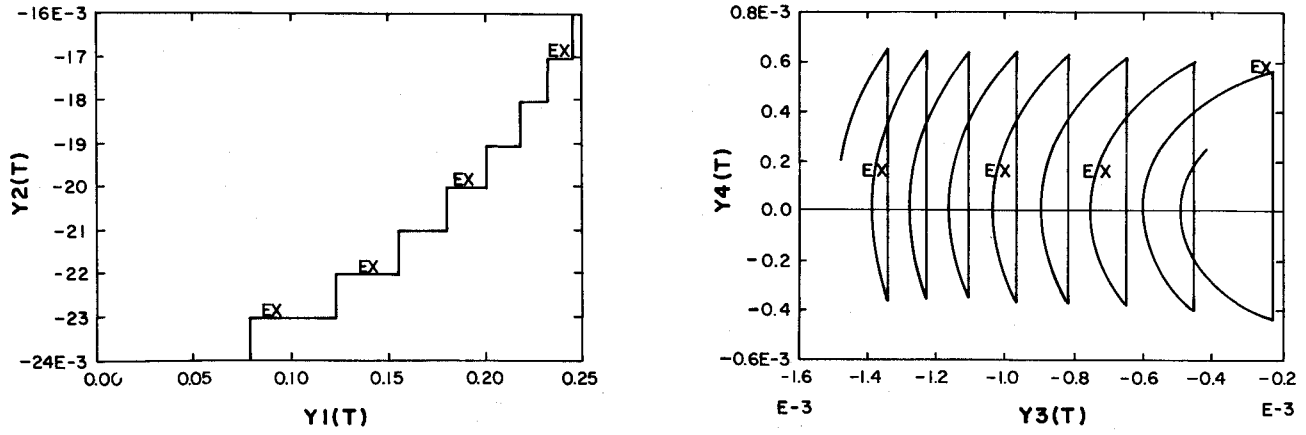

c) $t \in [79.97, 90.00]$ s

Fig. 6 State trajectories $y^a(.)$ and $y^{ex}(.)$ produced by the Vander Velde solution to problem 1 using the approximate (AP) or the exact (EX) solution to problem 2 for the data in Table 4.

Table 4 System parameters and initial state y_0 for Fig. 6

k	4	ω_1, rad/s	1
l	1	t_0	0
b_1	10	$y_1(t_0)$	25
c_{11}	0	$y_2(t_0)$	5
c_{21}	1	$y_3(t_0)$	5
c_{31}	0	$y_4(t_0)$	5
c_{41}	1	$n_{\max}$	8
um_1	1	θ^a, rad	0.7200152515
σ_1	0		

control. In Fig. 6, $y(t_0) = y_0$ was chosen with positive components and large $y_1(t_0)$ (the rigid-mode position coordinate) to simulate a worst-case, rapid-slewing maneuver of a single-axis nonrigid body. It and similar figures[2] for other cases show that:

1) During the transient, the greater $b_1 \cdot um_1$ is (i.e., the greater the penalty in the cost function for the use of control is), the slower the $y^a(.)$ and $y^{ex}(.)$ net motions toward the origin become and the longer they remain coincident, due to the smaller rate of fuel consumption and to the consequently smaller differences between the approximate and exact solutions to problem 2. Later, those trajectories separate and diverge, with $y^a(.)$ executing a smaller y_R excursion and an earlier arrival to steady state than $y^{ex}(.)$. This is due to the smaller (greater) competition between the exact solution to the rigid subproblem and the approximate (exact) solution to the undamped flexible subproblem for the determination of the relay input $d_1^a[y(t)]$, as characterized by the unbounded $d_R^o[y_R(t)]$ vs the bounded $d_{F1}^a[y_{F1}(t)]$ or unbounded $d_{F1}^o[y_{F1}(t)]$.

2) During the steady state, $y^a(.)$ describes what seems to be a limit cycle (whose existence was not proved theoretically) around the origin and symmetric with respect to **0**, but not with respect to any of its coordinate axes. Its y_R projection has two arcs close to the parabolic off/on switching lines of the exact solution to the constrained rigid subproblem, because there the function $d_R^o(y_R)$ is discontinuous and unbounded, causing $d_R^o[y_R(t)]$ to dominate $d_{F1}^a[y_{F1}(t)]$ until $w_R^o[y(t)] = J_R^o[y_R(t)]/J^a[y(t)]$ becomes sufficiently small. (In the Vander Velde controller for problem 1, the switching function that determines the control is formed as a linear combination of the individual constrained subproblem switching functions, each of which is weighted by the ratio of the cost associated with that subproblem to the total cost to complete the mission from the current state. The demands of each subproblem compete for the choice of control, which drives all the modes, when there are fewer controls than modes in the system model.) Its subsequent arcs show the alternate dominance or tie or even agreement between the two subproblems. Its dimensions vary inversely with $b_1 \cdot um1$.

On the other hand, $y^{ex}(.)$ never describes anything resembling a limit cycle. Instead, it does the following:

1) For small $b_1 \cdot um_1$, it keeps turning around the origin in an irregular pattern. Its y_{F1} projection frequently has two arcs close to the semicircular off/on switching lines adjacent to the origin of the exact solution to problem 2, because there the function $d_{F1}^o(y_{F1})$ is discontinuous and unbounded, causing $d_{F1}^o[y_{F1}(t)]$ to dominate $d_R^o[y_{R(t)}]$ until $w_{F1}^0[y(t)] = J_{F1}^o[y_{F1}(t)]/J^a[y(t)]$ becomes sufficiently small. This sometimes produces large excursions in its y_R projection. Conversely, the dominance of $d_R^o[y_R(t)]$ on $d_{F1}^o[y_{F1}(t)]$ also happens, resembling that of $d_R^o[y_R(t)]$ on $d_{F1}^a[y_{F1}(t)]$, but causing smaller excursions on its y_{F1} projection because this response is oscillatory whereas the rigid mode accelerates in one direction for constant control input. Hence, little improvement in the problem 1 solution is obtained.

2) For large $b_1 \cdot um_1$, it ends chattering very close to and toward the origin, the consequence of a chattering control with mean much smaller than um_1, reflecting the intense competition between subproblems. Its pattern is irregular, but confined to a neighborhood of **0** much smaller than the correspondent $y^a(.)$ final cycle. Hence, considerable improvement in the problem 1 solution is obtained.

All of this analysis suggests the following.

Conclusion 8. The improvements in the Vander Velde solution to problem 1 caused by substituting the exact solution to problem 2 for his approximate one seems considerable (negligible) in the large (small) $b_1 \cdot um_1$ case. The larger $b_1 \cdot um_1$ is, the slower $y^a(.)$ and $y^{ex}(.)$ move toward the origin and the later they separate. $y^a(.)$ executes a smaller y_R excursion and a faster transient than $y^{ex}(.)$, ending in a still-to-be-proved limit cycle whose dimensions vary inversely with $b_1 \cdot um_1$. However, $y^{ex}(.)$ ends in an irregular pattern that includes chattering (large y_R excursions) very close to (far from) the origin. So, in applications where this cannot happen, a small dead zone around **0** can suppress it. In situations similar to those mentioned in conclusion 2, a practical scheme is to use the approximate solution to problem 2 while y_{F1} is far from the origin; and switch to the exact one when y_{F1} becomes close to **0**.

Conclusions

In this paper, the exact solution to the problem of the weighted time/fuel optimal control of an undamped harmonic oscillator with one bounded control and any initial state was summarized. In it, the three determinant quantities for each of its extremal controls are: its final control, the first component of its final costate, and its final time. They determine its initial state with the help of m and n, i.e., the number of on and off arcs between the (m,n) arc and its origin. Its extremal controls exist, are normal, can be nonunique (but in a finite number), and can be determined by an algorithm based on its properties. Its optimal control exists, is normal, is unique, can also be determined by such algorithm, and seems to improve the final behavior of Vander Velde's designs for on/off controls of large space structures.

Acknowledgments

The author thanks Prof. Wallace E. Vander Velde of the Massachusetts Institute of Technology for his patience and guidance throughout his doctoral program. The dissertation includes the present results. He also thanks the overall support for that program provided by Conselho Nacional de Desenvolvimento Científico e Tecnológico and by Instituto de Pesquisas Espaciais both from República Federativa do Brasil.

References

[1]Vander Velde, W. E. and He, J., "Design of Space Structure Control Systems Using On-Off Thrusters," *Journal of Guidance, Control and Dynamics*, Vol. 6, Jan.–Feb. 1983, pp. 53–60.

[2]Souza, M. L. O., "On the Vander Velde Solution to the Problem of the Weighted Time-Fuel Optimal Control of a Flexible Spacecraft," Ph.D. Dissertation, Dept. of Aeronautics and Astronautics, Massachusetts Institute of Technology, Cambridge, MA, June 1985.

[3]Athans, M. and Falb, P., *Optimal Control: An Introduction to the Theory and Its Applications*, McGraw-Hill, New York, 1966.

[4]Ryan, E. P., *Optimal Relay and Saturating Control System Synthesis*, Peter Peregrinus, Stevenage, UK, 1982.

[5]Pontryagin, L. S., Boltyanskii, V. G., Gamkrelidze, R. V., and Mischenko, E. F., *The Mathematical Theory of Optimal Processes*, Wiley-Interscience, New York, 1962.

[6]Brown, M. E., "Rapid Slewing Maneuvers of a Flexible Spacecraft Using On/off Thrusters," Charles Stark Draper Laboratory Inc., Cambridge, MA, Rept. CSDL-T-825, Sept. 1983.

[7]Bushaw, D. W., "Differential Equations with a Discontinuous Forcing Term," Experimental Towing Tank, Stevens Institute of Technology, Hoeboken, NJ, Rept. 469, 1953.